

Protein Adsorption on Lipid Monolayers at their Coexistence Region

Roland R. Netz ^(1,*,**), David Andelman ⁽¹⁾ and H. Orland ^(2,***)

⁽¹⁾ School of Physics and Astronomy, Raymond and Beverly Sackler Faculty of Exact Sciences, Tel Aviv University, Ramat Aviv 69978, Tel Aviv, Israel

⁽²⁾ Service de Physique Théorique, CE-Saclay, 91191 Gif sur Yvette Cedex, France

(Received 2 October 1995, accepted 26 March 1996)

PACS.82.70.-y – Disperse systems

PACS.87.22.Bt – Membrane and subcellular physics and structure

PACS.64.75.+g – Solubility, segregation, and mixing; phase separation

Abstract. — We investigate theoretically the behavior of proteins as well as other large macromolecules which are incorporated into amphiphilic monolayers at the air-water interface. We assume the monolayer to be in the coexistence region of the “main” transition, where domains of the liquid condensed phase coexist with the liquid expanded background. Using a simple mean-field free energy accounting for the interactions between proteins and amphiphilic molecules, we obtain the spatial protein distribution with the following characteristics. When the proteins preferentially interact with either the liquid condensed or liquid expanded domains, they will be dissolved in the respective phase. When the proteins are energetically rather indifferent to the density of the amphiphiles, they will be localized at the line boundary between the (two-dimensional) liquid expanded and condensed phases. In between these two limiting cases, a delocalization transition of the proteins takes place. This transition is accessible by changing the temperature or the amount of incorporated protein. These findings are in agreement with recent fluorescence microscopy experiments. Our results also apply to lipid multicomponent membranes showing coexistence of distinct fluid phases.

1. Introduction

Monolayers of amphiphilic molecules spread on liquid surfaces have traditionally been studied as models for biological membranes [1, 2]. Such insoluble and monomolecular films made of suitable phospholipids or fatty acids are stable over a wide range of surface pressures and temperatures due to the strong reduction of the water surface tension and are called *Langmuir monolayers* [3]. In typical experiments, the amphiphiles are solubilized in a volatile solvent and placed on the air-water interface. As the solvent evaporates, the amphiphiles spontaneously spread and form a monolayer. When the insoluble film is then compressed (while keeping

(*) Author for correspondence (e-mail: netz@pauli.phys.washington.edu)

(**) *Present address:* Department of Physics, Box 351560, University of Washington, Seattle, WA 98195-1560, USA

(***) Also at: Groupe de Physique Statistique, Université de Cergy-Pontoise, 95806 Cergy-Pontoise Cedex, France

the temperature fixed), the lateral pressure can be measured as a function of the area per amphiphilic molecule in analogy to bulk isotherms.

Using film balance techniques [1–5], the following general picture emerged. When the extremely expanded film is compressed, it produces the liquid expanded phase (LE), which, at low enough temperatures, transforms upon further compression into the liquid condensed phase (LC). At much lower surface concentrations and at low enough temperatures, the monolayer undergoes a first-order transition into a gaseous phase. At very high lateral pressures, solidification occurs, as indicated by a discontinuity in the pressure-area isotherms. Subsequently, these systems were also studied using X-ray [6–9] and neutron [10] scattering techniques, indicating the existence of a large number of different condensed phases. In this paper we will be concerned only with the LE/LC transition. Therefore, we do not introduce appropriate order parameters needed to distinguish the different condensed phases [11].

The nature of the LE/LC transition has been the subject of much discussion [12]. It is analogous to the “main” transition in lipid bilayers [3], where domains of the LE and the LC phases have been shown to coexist over a wide range of lipid surface concentrations (or area per molecule). In this coexistence region, the condensed domains show a large variety of different shapes [13] and grow as the area per molecule is decreased, whereas the number of domains depends on the initial conditions and typically stays fixed. The isotherms in the coexistence region, however, were found to be non-horizontal, which led to the postulation of a limited cooperativity of this transition [4]. For the case of single-chain fatty acids, it was later shown that the isotherms approach zero slope as the material used is progressively purified [12].

On the theoretical side, the LE/LC transition has been modeled based on various microscopic pictures of the interaction between surfactant (or lipid) molecules including translational as well as internal degrees of freedom [14–18].

The biological function of membranes depends mostly on the incorporation of proteins and other macromolecules into the lipid layers. Functionality and efficiency of these inclusions depend crucially on microscopic details of the embedding in the lipid matrix, which can occur in different ways. Monolayers at the air-water interface are suitable for the study of the interaction between lipids and proteins, since they are rather well-defined and allow the control of independent thermodynamic parameters which are otherwise fixed in a bilayer membrane, like the area per molecule. Also, the observational techniques are well developed. Direct visualization of the phase behavior of monolayers can be obtained using fluorescence microscopy techniques. Here, a fluorescent dye probe is incorporated into the monolayer and its lateral distribution can be obtained from the analysis of fluorescence micrographs. Contrast in the images is obtained as a result of different dye solubility, fluorescence quantum yield, or molecular density of coexisting phases [19]. A complementary and recently developed technique is Brewster-angle microscopy, which allows imaging of a monolayer without the addition of fluorescent probes [20].

After injection of a water-soluble protein into the aqueous subphase, the surface tension typically decreases, indicating that the protein is at least partially incorporated into the monolayer [3, 21–23]. This is due to the protein affinity to the water/air interface. The specific type of this attraction is not well understood and probably is due in part to structural changes (denaturation) of the protein in the monolayer or at the water surface, associated with the unfolding of hydrophobic groups.

One of the striking experimental observations [22, 24] was that some proteins adsorb preferentially along the *boundary line* between the LE and LC domains when the monolayer is in the LE/LC coexistence region. These observations were made for fluorescently labeled small proteins, such as *concanavalin A* [24] or *streptavidin* [22], interacting with phospholipid monolayers. These experimental findings motivated our present theoretical study.

In the following, we describe a simple model, which (i) assumes the LE/LC transition to be a simple first-order condensation transition, yielding coexisting domains for temperatures below the critical temperature, and (ii) includes the effect of proteins which are adsorbed into the monolayer. Assuming that the proteins are completely incorporated into the monolayer, this simplistic model leads to an entropic force which tends to localize the protein at the boundary between LE and LC domains. Depending on the energetic preference of the protein for the LE or LC phase, the protein will be either dissolved in the LE or in the LC domain, or, if there is no pronounced preference, will be localized at the boundary.

Phase separation in amphiphilic layers is also observed for freely suspended multicomponent bilayers [2]. Here, the coexisting phases are distinguished by their compositions. The most important examples include mixtures of phospholipids with cholesterol [25] and mixtures of different phospholipids [26], and in both cases the coexisting phases are in a fluid state. These phenomena are of great biological interest since biological membranes are always multicomponent mixtures and lateral organization into domains is supposed to play an important functional role. We note that our results apply directly to these situations as well, although we will limit our terminology to the situation of coexisting dense and dilute phases for one-component systems at the air-water interface. For the case of freely suspended membranes, our findings imply a simple mechanism for the localization of integral membrane proteins along the one-dimensional boundary between coexisting domains. The resulting enrichment of proteins might be a prerequisite for proper biological function in certain cases.

In the following sections we formulate the model (Sect. 2), inspect the minima of the free energy (Sect. 3), solve the corresponding Euler-Lagrange equations in the coexistence region (Sect. 4), and calculate profiles both for the lipid and the (coupled) protein densities (Sect. 5). From the profiles we generate a general phase diagram featuring localized, semi-localized and delocalized protein phases. We also calculate the total amount of adsorbed protein, the protein excess Γ (Sect. 6), and the line tension τ of the LE-LC line interface (Sect. 7). It turns out that the line tension is strongly reduced by the adsorption of proteins. A finite solubility of the proteins in the subphase is taken into account in Section 8. Finally, the connection to experimentally measurable quantities, such as the surface pressure Π , is made in Section 9.

2. The Mixed Lipid and Protein Free Energy

Consider the air-water interface with proteins, lipid molecules, and artificial “vacancies”, with area fractions ϕ_P , ϕ_L , and ϕ_V , respectively, satisfying $\phi_P + \phi_L + \phi_V = 1$. The vacancies are introduced in order to allow for independent variations of the protein and lipid concentrations, hence making coexistence of dilute and condensed regions of the monolayer possible. Inscribing the system on a lattice, with a lattice constant corresponding to the size of a lipid molecule, the free energy of mixing per lattice site within a mean field theory can be written for the three-component mixture as a sum of the enthalpy and entropy of mixing, $\mathcal{F} = \mathcal{U} - T\mathcal{S}$. The enthalpy of mixing includes all pair-wise interactions between the three species:

$$\mathcal{U}/T = E_{LL}\phi_L^2 + E_{VV}\phi_V^2 + E_{PP}\phi_P^2 + E_{LV}\phi_L\phi_V + E_{PL}\phi_P\phi_L + E_{PV}\phi_P\phi_V \quad (1)$$

and the E_{ij} are the dimensionless interaction parameters for all possible pairs. The entropy of mixing is related to the total number Ω of distinct microscopic configurations

$$\mathcal{S} = \frac{\log \Omega}{N} \quad (2)$$

where N is the total number of lattice sites and the Boltzmann constant is set to unity ($k_B = 1$). In the random-mixing approximation,

$$\Omega = \frac{(N(\phi_L + \phi_V + \phi_P/\alpha))!}{(N\phi_P/\alpha)!(N\phi_L)!(N\phi_V)!} \quad (3)$$

where the constant $\alpha > 1$ denotes the ratio between the compact area occupied by a protein molecule and a lipid molecule at the interface. The above expression is a modification of the usual Flory-Huggins formula for the entropy of mixing, and yields the correct behavior in the limit $\phi_P \rightarrow 0$ (see Sect. 9). It is exact for the one-dimensional case. Using Stirling's formula in the thermodynamic limit, defined by $N \rightarrow \infty$, the expression for \mathcal{S} can be simplified

$$\mathcal{S} = -\phi_L \log(\phi_L) - \phi_V \log(\phi_V) - \frac{\phi_P}{\alpha} \log\left(\frac{\phi_P}{\alpha}\right) + \left(1 - \phi_P + \frac{\phi_P}{\alpha}\right) \log\left(1 - \phi_P + \frac{\phi_P}{\alpha}\right) \quad (4)$$

It is convenient to define the thermodynamic potential

$$\mathcal{G}/T = \mathcal{F}/T - \mu_P \phi_P - \mu_L (\phi_L - \phi_V) \quad (5)$$

where the chemical potentials μ_P and μ_L are coupled to the protein concentration ϕ_P and the difference between the lipid and vacancy concentrations, $\phi_L - \phi_V$, respectively.

In (1)-(5), long-range interactions between the proteins, such as electrostatic forces, are not taken into account. In addition, the free energy of mixing assumes a confinement of the protein and lipid to the two-dimensional plane of the air-water interface. In fact, the variation of the protein concentration perpendicular to the monolayer in the subphase can be taken into account approximately and leads to a renormalization of the parameters of the two-dimensional model, as shown in Section 8.

The lipid order parameter η , corresponding to the density of lipid molecules, can be written as

$$\eta \equiv \phi_L - \phi_V \quad (6)$$

Using that $\phi_P + \phi_L + \phi_V = 1$, and defining the protein concentration as $\phi \equiv \phi_P$, the free energy \mathcal{F} and the potential \mathcal{G} can be rewritten as

$$\begin{aligned} \mathcal{F}/T &= -(J + 1/2)\eta^2 + L\phi^2 + \lambda\eta\phi \\ &+ (1 + \eta - \phi) \log[(1 + \eta - \phi)/2]/2 + (1 - \eta - \phi) \log[(1 - \eta - \phi)/2]/2 \\ &+ \phi \log[\phi/\alpha] - (1 - \phi + \phi/\alpha) \log[1 - \phi + \phi/\alpha] \end{aligned} \quad (7)$$

and

$$\mathcal{G}/T = \mathcal{F}/T - \mu_\eta \eta - (\mu + \log 2)\phi \quad (8)$$

where constant terms have been omitted and linear terms in η and ϕ have been dropped out from \mathcal{F} for convenience. They merely contribute a constant shift to μ and μ_η in \mathcal{G} . The reduced interaction parameters: J , L , μ and λ are related to the original E_{ij} and μ_P in the following way

$$-J \equiv \frac{1}{4}(E_{LL} + E_{VV} - E_{LV}) + \frac{1}{2} \quad (9)$$

$$L \equiv \frac{1}{4}(E_{LL} + E_{VV} + E_{LV}) + E_{PP} - \frac{1}{2}(E_{PL} + E_{PV}) \quad (10)$$

$$\lambda \equiv -\frac{1}{2}(E_{LL} - E_{VV} - E_{PL} + E_{PV}) \quad (11)$$

$$\mu \equiv \mu_P + \frac{1}{2}(E_{LL} + E_{VV} + E_{LV} - E_{PL} - E_{PV}) - \log 2 \quad (12)$$

The constant $\log 2$ appears in the definition of μ in order to render the simplified expression (13) in a simpler form.

The above expression for \mathcal{G} is studied in Section 3 for different values of the various parameters and the corresponding bulk phase-diagrams are obtained. For the study of protein profiles, one can further simplify this expression. First, for small values of the order parameters, *i.e.*, relatively close to the critical point of demixing of the lipid and for small protein concentrations, it is legitimate to expand the free energy of mixing up to order $\mathcal{O}(\eta^4)$ and $\mathcal{O}(\phi^2)$. In addition, since typical proteins occupy a much larger area than lipids, the area ratio is in the range of $\alpha \sim 50 - 100$, and the protein entropy terms (of order $1/\alpha$) can be neglected in (7). The validity of the latter ($\alpha \rightarrow \infty$) approximation will be reexamined in Section 3 [27]. With these simplifications, the approximated free energy density can be written as

$$\mathcal{F}^0/T = -J\eta^2 + \frac{1}{12}\eta^4 + L\phi^2 + \lambda\eta\phi + \frac{1}{2}\eta^2\phi \quad (13)$$

where the simplified thermodynamic potential using (8) is given by $\mathcal{G}^0/T = \mathcal{F}^0/T - \mu\phi - \mu_\eta\eta$. The free energy density (13) needs some further discussion. Coexistence between dense ($\eta > 0$) and dilute regions ($\eta < 0$) requires that $J > 0$ and a positive fourth-order term η^4 is needed to stabilize the free energy. The protein itself is assumed not to be close to any phase transition. Hence $L > 0$ and no higher order terms in ϕ are needed. We include in the expansion only the two lowest coupling terms between the protein and lipid concentrations. The first is the bilinear coupling $\eta\phi$ and has an enthalpic origin. It reflects the overall preference of the protein to more condensed ($\lambda < 0$) or more dilute ($\lambda > 0$) regions of the lipid monolayer. The second coupling is the symmetric $\eta^2\phi$ term, which is invariant under $\eta \rightarrow -\eta$ transformation and provides the driving force for the localization of proteins at the LE-LC interface. In our mean-field model, taking into account only pair interactions, this coupling has a purely entropic origin. More generally, it can also include interaction terms of higher-order in a virial expansion. Finally, the higher-order coupling terms $\eta^2\phi^2$ and $\eta^4\phi$ are not considered here since we try to investigate the most simple and yet non-trivial type of coupling. A similar free energy coupling has been introduced in the context of polymer adsorption at liquid-liquid interfaces, where in analogy the polymer adsorbs preferentially at the interface from the bulk solution [28].

For the case where the proteins in the monolayer are in equilibrium with a solution of proteins in the aqueous subphase, the protein chemical potential μ corresponds to the free energy of adsorbing proteins from the subphase into the monolayer and depends on the concentration of proteins in the subphase; this is discussed in Section 8. Since we consider an insoluble (Langmuir) monolayer, similar considerations do not apply to the chemical potential μ_η of the lipid order parameter η . In fact, μ_η will be uniquely determined by the requirement of coexistence between dense and dilute lipid regions. For proteins which are *insoluble* in the subphase, the chemical potential μ acts as a Lagrange multiplier fixing the total amount of protein in the monolayer, which is a conserved quantity in this situation.

In the LE/LC two-phase region, obtained for $J > 0$, one finds experimentally [3] domains of typically circular shape of LC phase immersed in a background of LE phase. Since the domains are rather large ($\sim 10 - 100 \mu\text{m}$), we neglect the shape of the line boundary between the LC and LE regions and assume variation of the lipid concentration only along one spatial direction (the x direction) and translational invariance along the perpendicular direction. The free energy γ per unit length of this line boundary (related to the line tension τ of the interface as calculated in Sect. 7) is given by

$$\gamma = \int_{-\infty}^{\infty} \mathcal{I} dx \quad (14)$$

where the free energy density \mathcal{I} includes contributions associated with spatial variations of the concentrations. Defining the “stiffness coefficients” g_ϕ and g_η for the protein and lipid concentration profiles, respectively, the free energy density \mathcal{I} is given by

$$\mathcal{I} = \mathcal{G}/T + \frac{1}{2}g_\phi \left(\frac{d\phi}{dx} \right)^2 + \frac{1}{2}g_\eta \left(\frac{d\eta}{dx} \right)^2 \quad (15)$$

In the next section we study the bulk phase diagram based on the thermodynamic potential (8). In the subsequent sections we use the simplified expression (13) and determine the concentration profiles $\phi(x)$ and $\eta(x)$ by applying a variational principle to the free energy functional γ .

3. The Phase Diagram

The phase diagram as a function of the chemical potentials μ_η and μ can be obtained from the thermodynamic potential (8) by minimizing \mathcal{G} with respect to the order parameters η and ϕ in the two-phase coexistence region [29]. The coexisting solutions, denoted by (η_1, ϕ_1) and (η_2, ϕ_2) , are determined from the equations

$$\mu_\eta = \left. \frac{\partial \mathcal{F}}{\partial \eta} \right|_{\eta_1, \phi_1} = \left. \frac{\partial \mathcal{F}}{\partial \eta} \right|_{\eta_2, \phi_2} = \frac{\mathcal{F}(\eta_1, \phi_1) - \mathcal{F}(\eta_2, \phi_2)}{\eta_1 - \eta_2} \quad (16)$$

$$\mu + \log 2 = \left. \frac{\partial \mathcal{F}}{\partial \phi} \right|_{\eta_1, \phi_1} = \left. \frac{\partial \mathcal{F}}{\partial \phi} \right|_{\eta_2, \phi_2} \quad (17)$$

which correspond to a common-tangent construction. These equations can be easily solved numerically. In order to estimate the role of the protein-lipid area ratio, α , and to compare the results with the calculations presented in the next section based on the simplified expression (13), where $\alpha \rightarrow \infty$, we restrict the numerical analysis to the values $J = 1/10$ and $L = 10$. The small value of J means that one is close to the critical point of the lipid phase separation, and the expansion in powers of η , leading to (13), is appropriate. The large value of L means that the protein concentration is rather small everywhere and can be treated as a small perturbation. We will need this assumption for the analytic solution of the Euler-Lagrange equations in Section 4. The parameter α will be scanned in a rather wide range. With this choice of L and J , it is clear that the simplified free energy expression (13) is asymptotically obtained for $\alpha \rightarrow \infty$.

The protein concentrations in the coexisting dense and dilute lipid regions scan a whole range of different values, depending on the values of the remaining parameters μ and λ , but are strictly bounded below by $\sim \exp(-\alpha)$. In contrast, the simplified free energy expression (13) has solutions with non-zero and strictly zero protein concentrations, because of the $\alpha \rightarrow \infty$ limit. It therefore allows for straightforward classification of the bulk protein ordering into a phase with finite protein concentration and a phase with no proteins at all. We need a similar criterion for the case of the full free energy expression (7) with α finite, allowing us to distinguish in a categorical manner the presence of proteins from the absence of proteins, even in the inevitable presence of a protein concentration exponentially small in α . We adopt the simple criterion which consists of calculating the Laplacian of the protein concentration in the parameter space (μ, λ) ,

$$\frac{\partial^2 \phi_i}{\partial \mu^2} + \frac{\partial^2 \phi_i}{\partial \lambda^2} \quad (18)$$

in the two coexisting phases ϕ_1 and ϕ_2 . This scalar quantity shows a pronounced line of maxima in the parameter space, separating two phases with small and large concentrations of proteins.

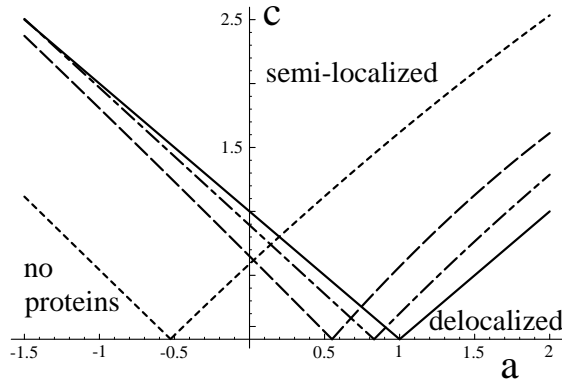


Fig. 1. — Bulk phase diagram for $L = 10$, $J = 1/10$, and for $\alpha = 10$ (short dashes), 50 (long dashes), and 200 (long-short dashes) as a function of the rescaled chemical potential parameter a and the interaction parameter c . The solid lines denote the phase boundaries for the limiting case $\alpha \rightarrow \infty$. In the delocalized-phase region the protein concentration in the dense and dilute lipid regions is finite; in the so-called “semi-localized” region only the dilute lipid region contains proteins (for negative values of c only the dense lipid region contains proteins), and in the region denoted by “no proteins” the protein concentration is very small ($\sim \exp[-\alpha]$) in both coexisting lipid regions. In part of the “no protein” region, the solution of the Euler-Lagrange equations gives a new localized protein distribution in the neighborhood of the LE/LC boundary, see Figure 2.

The position of this ridge is determined numerically and defined as the boundary between the two phases rich and devoid of proteins, respectively, for each solution ϕ_i . The result of this operation leads to three distinct phase regions and is shown in Figure 1 for the values $\alpha = 10$, 50, and 200. Anticipating the definitions (28) and (30), we present the results in terms of the rescaled variables $a \equiv \mu/(3J)$ and $c \equiv \lambda/\sqrt{3J/2}$. The results obtained for $\alpha = \infty$ are denoted by solid lines. In the region denoted “no proteins” both protein concentrations ϕ_1 and ϕ_2 are very small (exponentially in $-\alpha$); in the region “semi-localized” only one concentration is small while the other is finite (distinguished by the criterion described above), and in the region “delocalized” both phases have finite protein concentrations.

In the next section we will calculate the protein profile explicitly and, in addition, obtain a “localized” phase. This phase cannot be distinguished from the “no protein” phase by just looking at the bulk free energy. In fact, in this phase there is a finite protein concentration only at a finite distance from the boundary between the LE and LC regions. As one can see from Figure 1, the phase boundary for $\alpha = 50$ (long dashes) is already fairly close to the asymptotic boundary ($\alpha \rightarrow \infty$, solid line), so that neglecting the protein entropy is already a good approximation for moderately large macromolecules.

4. Euler-Lagrange Equations

In this section we calculate the protein concentration profile based on the free energy expression (15). Minimization of the line free energy γ (14) leads to the Euler-Lagrange equations (denoting $d\phi/dx$ by ϕ' , etc.)

$$\frac{\partial \mathcal{I}}{\partial \eta} - \frac{d}{dx} \frac{\partial \mathcal{I}}{\partial \eta'} = 0 \quad (19)$$

$$\frac{\partial \mathcal{I}}{\partial \phi} - \frac{d}{dx} \frac{\partial \mathcal{I}}{\partial \phi'} = 0 \quad (20)$$

Using the full free energy of mixing (7), one obtains two coupled second-order and non-linear differential equations of the form

$$-\mu_\eta - (2J + 1)\eta + \lambda\phi + \frac{1}{2} \log \left(\frac{1 + \eta - \phi}{1 - \eta - \phi} \right) = g_\eta \frac{d^2 \eta}{dx^2}$$

$$-\mu - \log 2 + 2L\phi + \lambda\eta + \frac{1}{2} \log \left(\frac{4(1 - \phi)^2}{(1 + \eta - \phi)(1 - \eta - \phi)} \right) + \frac{1}{\alpha} \log \left(\frac{\phi}{1 - \phi} \right) = g_\phi \frac{d^2 \phi}{dx^2}$$

For the actual calculation of concentration profiles, we will use the simplified free energy expression (13), leading to the more compact expressions (which are expansions in η and ϕ)

$$-\mu_\eta - 2J\eta + \frac{1}{3}\eta^3 + \lambda\phi + \eta\phi = g_\eta \frac{d^2 \eta}{dx^2} \quad (21)$$

$$-\mu + 2L\phi + \lambda\eta + \frac{1}{2}\eta^2 = g_\phi \frac{d^2 \phi}{dx^2} \quad (22)$$

These are the same equations that were considered by Halperin and Pincus in the context of polymer adsorption at liquid-liquid interfaces [28].

Instead of solving (21), (22) numerically, we recall that for large values of L we can treat the protein area fraction as a small parameter. As a zeroth-order approximation, we neglect the terms depending on ϕ in (21) and obtain as a solution the lipid order parameter profile $\eta_0(x)$ in the absence of proteins. This profile is then inserted into (22), yielding the protein profile $\phi(x)$. The validity of this approach, namely solving the equation (21) while neglecting the coupling between η and ϕ and inserting the solution into equation (22), is critically examined in Appendix B. There, it is found that this approximation indeed corresponds to the first term in an expansion, in which the protein concentration functions as the expansion parameter and which therefore is valid for small protein concentrations.

To proceed, setting $\phi = 0$ in (21) leads to

$$\eta_0(x) = \eta_\infty \tanh(x/\xi_\eta) \quad (23)$$

with the definitions

$$\eta_\infty \equiv \sqrt{6J} \quad (24)$$

$$\xi_\eta \equiv \sqrt{g_\eta/J} \quad (25)$$

This is the solution of the usual 4th order Ginzburg-Landau free energy expansion and is strictly valid here only for the pure lipid. The lipid order parameter varies between $+\eta_\infty$ for $x \rightarrow \infty$ and $-\eta_\infty$ for $x \rightarrow -\infty$, and its width is characterized by the correlation length ξ_η . The chemical potential μ_η is zero in the approximation employed above. The origin is chosen as the symmetric point between the liquid condensed phase ($x > 0$) and the liquid expanded phase ($x < 0$). Defining a rescaled length $u \equiv x/\xi_\eta$ and a rescaled protein density $\Phi(x) \equiv 4L\phi(x)/(\eta_\infty)^2$, the second differential equation (22) is reduced to

$$\Phi(u) - h(u) = b^2 \frac{d^2 \Phi(u)}{du^2} \quad (26)$$

with the inhomogeneous term $h(u)$ given by

$$h(u) \equiv a - \tanh^2(u) - c \tanh(u) \quad (27)$$

The remaining rescaled parameters are

$$a \equiv \frac{2\mu}{(\eta_\infty)^2} = \frac{\mu}{3J} \quad (28)$$

$$b^2 \equiv \frac{Jg_\phi}{2Lg_\eta} = \frac{\xi_\phi^2}{\xi_\eta^2} \quad (29)$$

$$c \equiv \frac{2\lambda}{\eta_\infty} = \frac{\lambda}{\sqrt{3J/2}} \quad (30)$$

The parameter $a \sim \mu$ is the rescaled chemical potential, b is the relative stiffness of the lipid concentration profile compared to the protein concentration profile, and $c \sim \lambda$ measures the preference of the proteins for the dense ($c < 0$) or dilute ($c > 0$) lipid domains. The correlation length of the protein distribution is defined by $\xi_\phi \equiv \sqrt{g_\phi/2L}$.

The general solution of the second order differential equation (26) can be written as

$$\Phi(u) = A \sinh(u/b) + B \cosh(u/b) + a - \Phi_1(u)/b - c\Phi_2(u)/b \quad (31)$$

where the functions $\Phi_1(u)$ and $\Phi_2(u)$ are given in Appendix A. The constants A and B have to be determined in accord with the boundary conditions.

5. Protein Distribution

5.1. SOLUTION FOR THE CASE $b = 0$. — It is instructive to treat first the limiting case where the stiffness of the protein distribution vanishes, *i.e.*, $g_\phi = 0$ and $\xi_\phi = 0$. Then, one has $b = 0$ and the solution of (26) is trivially given by $\Phi(u) = h(u)$. This leads to the protein distribution

$$\Phi^0(u) = \begin{cases} h(u) & \text{for } h(u) \geq 0 \\ 0 & \text{for } h(u) < 0 \end{cases} \quad (32)$$

where the restriction to a finite range in u follows since the protein concentration $\Phi^0(u)$ has to be positive. In fact, for $b = 0$, only for $h(u) \geq 0$ the protein distribution is correctly described by the differential equation (26); inspection of the free energy density \mathcal{I} in the limit $\alpha \rightarrow \infty$ shows that the value of $\Phi(u)$ which minimizes \mathcal{I} for $h(u) < 0$ is given by $\Phi(u) = 0$. This failure of the variational methods used in deriving (26) is due to the fact that one requires $\Phi(u)$ to be positive in the limit of very large proteins, $\alpha \rightarrow \infty$.

Hereafter, we choose $c \geq 0$ with no loss of generality, since the problem defined by (26) and (27) is symmetric under a simultaneous inversion of c and u ($c \rightarrow -c$ and $u \rightarrow -u$). Using the asymptotic behavior of $h(u)$,

$$h(u) = \begin{cases} a - 1 + c & \text{for } u \rightarrow -\infty \\ a - 1 - c & \text{for } u \rightarrow +\infty \end{cases} \quad (33)$$

the following classification emerges: (i) For $a \leq 1 - c$, the protein distribution vanishes both for positive and negative values of u at a sufficiently large but finite distance from the interface (which is located at $u = 0$); one actually obtains a nonvanishing, *localized* distribution of proteins provided that $h(u) > 0$ for some range of u , but this cannot be seen from the bulk

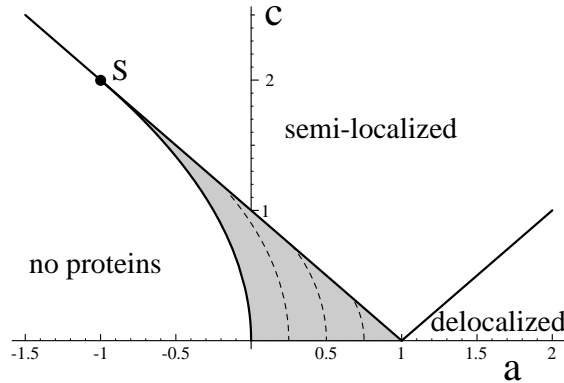


Fig. 2. — Phase diagram for general protein stiffness b , valid in the limit of large proteins, $\alpha \rightarrow \infty$, as a function of the protein chemical potential a and protein-lipid interaction parameter c . The shaded area denotes the localized regime, in which the protein distribution is localized at the boundary between dense and dilute lipid regions. The special point S is the limiting localized case where the maximum of the protein distribution is infinitely far away from the interface between the liquid condensed and liquid expanded phases. The broken lines denote lines of constant excess protein Γ calculated for the special case $b = 0$. The phase diagram is symmetric with respect to the a axis ($c = 0$ line).

behavior; (ii) for $1 - c < a \leq 1 + c$, the distribution is *semi-localized* and vanishes only for sufficiently large positive values of u and stays finite as $u \rightarrow -\infty$, and (iii) for $a > 1 + c$ the distribution is *delocalized* and stays finite in both limits $u \rightarrow \pm\infty$. These three regimes are in accord with the $\alpha \rightarrow \infty$ limit of the phase diagram shown in Figure 1.

An additional observation can be made for $c \leq 2$, where $h(u)$ has one maximum located at

$$u_{\max} = -\tanh^{-1}(c/2) \quad (34)$$

with a height

$$h(u_{\max}) = a + c^2/4 \quad (35)$$

(in the limit $c \rightarrow 2$ one obtains $u_{\max} \simeq \log(2-c)/2$). Consequently, for $c \leq 2$, the line defined by $a = -c^2/4$ marks the border between a fourth regime where the protein distribution vanishes identically (for $a \leq -c^2/4$) and the regime where this distribution is non-zero (for a finite distance from the boundary between dense and dilute lipid regions). Figure 2 summarizes these borderlines in a phase diagram, which is in fact valid also for $b \neq 0$, as will be discussed in the next subsection. The localized regime is shaded in gray and ends at a special point S , at which the maximum of the protein distribution is at infinity; as pointed out before, there is an overall symmetry around the a -axis ($c = 0$).

The effective correlation length ξ_{eff} for the proteins in the localized regime can be estimated from the curvature of $\Phi^0(u)$ at the maximum u_{\max} ,

$$\xi_{\text{eff}}^{-2} \equiv -h''(u_{\max}) = 2(1 - c^2/4)^2 \quad (36)$$

This length diverges as one approaches the special point S , where the distribution becomes indefinitely broad.

5.2. SOLUTION FOR $b > 0$ — GENERAL CONSIDERATIONS. — On physical grounds, the solution for non-zero b , *i.e.*, for a finite stiffness of the protein distribution, has to coincide

with the solution found for $b = 0$ in the preceding section very far from the interface located at $u = 0$. This leads to the general boundary condition

$$\Phi(u) = \Phi^0(u) \quad \text{for } u \rightarrow \pm\infty \quad (37)$$

where $\Phi^0(u)$ is given by (32) and the general solution $\Phi(u)$ is defined to be the concentration profile which minimizes the free energy functional (14). In the following, we discuss the properties of the general solution $\Phi(u)$ separately for the four regions distinguished in Figure 2.

i) In the delocalized case, the boundary conditions (37) occurring at infinity together with the differential equation (26) valid for the entire $(-\infty, \infty)$ range in u are sufficient to determine the distribution $\Phi(u)$.

For the other cases, the boundary conditions (37) have to be supplemented by additional conditions at finite values of u ; the distribution $\Phi(u)$ is described by (26) only in a finite interval of u .

ii) In the case where $h(u) < 0$ for all u , it follows from the requirement $\Phi(u) \geq 0$ that $\Phi(u) - h(u) > 0$ and thus all possible solutions of (26) have strictly positive curvature as can be seen by looking at (26). The boundary conditions (37), which imply that $\Phi(u) = 0$ as $u \rightarrow \pm\infty$, can not be satisfied for any non-vanishing solution of (26). Consequently, the protein distribution which minimizes the free energy is given identically by $\Phi(u) = 0$. This vanishing solution was also found for $b = 0$.

iii) When $h(u)$ is positive in some finite interval of u but negative for $u \rightarrow \pm\infty$, all solutions of (26) which are positive definite everywhere have positive curvature for $u \rightarrow \pm\infty$ and are not compatible with the boundary conditions as given by (37). This merely reflects the fact that (26) describes the distribution $\Phi(u)$ only in the finite interval $u_1 \leq u \leq u_2$, in which $\Phi(u) > 0$. The same was found to be true for $b = 0$ in the last section. From (37) in combination with (32), $\Phi(u)$ has to vanish for $u \rightarrow \pm\infty$, and can be positive for finite u . As follows from minimizing the free energy functional γ (14), the solution $\Phi(u)$ has to be smooth everywhere and thus fulfills $\Phi(u) = \Phi'(u) = 0$ at the two boundaries $u = u_1$ and $u = u_2$.

Now the following statements can be made: a) There have to be intervals of u where $\Phi(u)$ has negative curvature in order to fulfill the boundary conditions $\Phi(u) = 0$ at $u = u_1$ and $u = u_2$; b) close to the boundaries $u = u_1$ and $u = u_2$, the curvature has to be positive in order to fulfill $\Phi'(u) = 0$ at $u = u_1$ and $u = u_2$; c) consequently, the solution $\Phi(u)$ crosses $h(u)$ at two values of u inside the region bounded by $u = u_1$ and $u = u_2$, at which the curvature of $\Phi(u)$ vanishes; this can be seen from (26). It follows that the boundaries u_1 and u_2 do not coincide, which means that the protein distribution $\Phi(u)$ does not vanish identically. We conclude that whenever the distribution $\Phi^0(u)$ does not vanish for $b = 0$, it is non-vanishing for any $b \neq 0$. Note that it is actually possible to construct a solution $\Phi(u)$ in accord with the boundary conditions at u_1 and u_2 since the general solution (31) has two adjustable parameters A and B .

iv) For the semi-localized case, the boundary condition (37) applies to the solution of (26) for $u \rightarrow -\infty$ only. The protein distribution is non-zero in the u interval $(-\infty, u_2)$ and the boundary value u_2 satisfies $\Phi(u_2) = \Phi'(u_2) = 0$.

Putting together these arguments for the different regimes, it follows that the phase diagram in Figure 2 is valid for general $b > 0$.

5.3. BOUNDARY CONDITIONS. — In the following, we specify the boundary conditions for general b for the three different cases showing non-vanishing protein distributions:

In the delocalized regime, the boundary conditions obtained from (37), (33), and (32) are

$$\Phi(\pm\infty) = h(\pm\infty) = a - 1 \mp c \quad (38)$$

These boundary conditions determine the coefficients A and B of the general solution (31). In the semi-localized regime, one has the conditions

$$\Phi(-\infty) = h(-\infty) = a - 1 + c \quad (39)$$

and

$$\Phi(u_2) = \Phi'(u_2) = 0 \quad (40)$$

which determine the position of the boundary value, u_2 , and the coefficients A and B . In the localized regime, one has

$$\Phi(u_1) = \Phi'(u_1) = 0 \quad (41)$$

$$\Phi(u_2) = \Phi'(u_2) = 0 \quad (42)$$

Here, the boundary conditions determine u_1 , u_2 , A , and B . In what follows, we always assume that $u_1 \leq u_2$, with no restrictions on the generality.

In the following, we present explicit protein profiles $\Phi(u)$ for the limiting cases $b = 0$ and $b = 1$. The latter value corresponds to the case where the correlation lengths of the lipid and protein concentration profiles are equal, $\xi_\eta = \xi_\phi$. Also, for $b = 1$, the general solution of the protein profile as given in Appendix A can be written in a simpler analytical form.

5.3.1. Delocalized Regime. — For $b = 1$, the coefficients are determined to be $B = \pi/2 - 2$ and $A = c(1 - \pi/2)$; the protein distribution, given by (31), then reads

$$\Phi(u) = a - 2 + 2 \tan^{-1}[\tanh(u/2)](c \cosh u - \sinh u) + \pi(\cosh u - c \sinh u)/2 \quad (43)$$

Using the equalities

$$\tan^{-1}[\tanh(u/2)] = \tan^{-1}[e^u] - \pi/4 = \pi/4 - \tan^{-1}[e^{-u}] \quad (44)$$

the protein distribution can be rewritten as

$$\Phi(u) = a - 2 + \pi e^u(1 - c)/2 + 2 \tan^{-1}[e^u](c \cosh u - \sinh u) \quad (45)$$

or

$$\Phi(u) = a - 2 + \pi e^{-u}(1 + c)/2 - 2 \tan^{-1}[e^{-u}](c \cosh u - \sinh u) \quad (46)$$

in accord with the limiting values $\Phi(u) = a - 1 \pm c$ for $u \rightarrow \mp\infty$.

5.3.2. Semi-Localized Regime. — For $b = 1$, the boundary condition at $u = -\infty$ leads to the relation $A = 2 + B + c - \pi(1 + c)/2$. The protein distribution can be written as

$$\Phi(u) = a - 2 + e^u(B + 2 - c\pi/2) + 2 \tan^{-1}[e^u](c \cosh u - \sinh u) \quad (47)$$

which indeed satisfies the boundary condition as given by (39). The coefficient B and u_2 are in turn determined by the second boundary condition (40).

5.3.3. Localized Regime. — For general b , the boundary conditions (41) and (42) can be cast in a more explicit form. Defining

$$\cosh(u/b)\Phi(u)/b - \sinh(u/b)\Phi'(u) = B/b + \rho(u) \quad (48)$$

with

$$\rho(u) \equiv \cosh(u/b)(a/b - \Phi_1(u) - c \Phi_2(u)) + b \sinh(u/b)(\Phi_1'(u) + c \Phi_2'(u)) \quad (49)$$

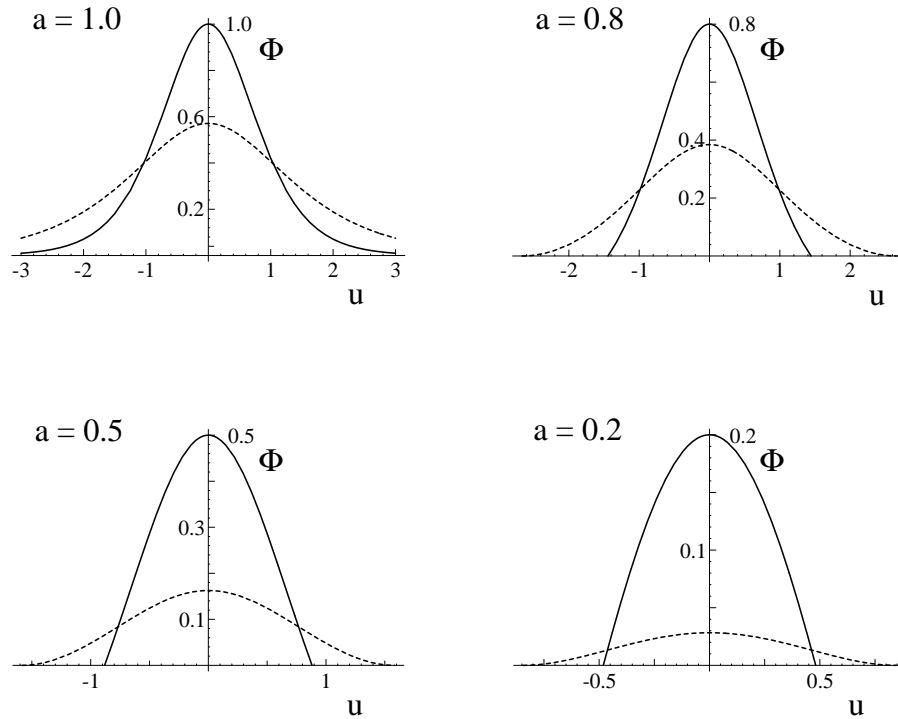


Fig. 3. — Protein distributions for the symmetric case defined by vanishing lipid-protein interaction, $c = 0$, for different values of the protein chemical potential a ; solid lines denote vanishing protein stiffness, $b = 0$, and broken lines denote $b = 1$.

and

$$\sinh(u/b)\Phi(u)/b - \cosh(u/b)\Phi'(u) = -A/b + \kappa(u) \tag{50}$$

with

$$\kappa(u) \equiv \sinh(u/b)(a/b - \Phi_1(u) - c \Phi_2(u)) + b \cosh(u/b)(\Phi'_1(u) + c \Phi'_2(u)) \tag{51}$$

leads to the equations

$$-B/b = \rho(u_1) = \rho(u_2) \tag{52}$$

$$A/b = \kappa(u_1) = \kappa(u_2) \tag{53}$$

Equations (48)-(51) have to be solved simultaneously in order to determine u_1 , u_2 , A , and B . For the case $b = 1$, the functions $\rho(u)$ and $\kappa(u)$ take the simpler form

$$\rho(u) = (a - 2) \cosh u + 2 + \tanh u \sinh u + 2c \tan^{-1}[\tanh(u/2)] - c \sinh u \tag{54}$$

$$\kappa(u) = (a - 1) \sinh u + 2 \tan^{-1}[\tanh(u/2)] + c(1 - \cosh u) \tag{55}$$

In the remainder of this section, we present protein profiles calculated from the above equations for several values of the three parameters a , b , and c . Figure 3 shows protein distributions for four different values of a and for the two simple cases $b = 0$ (solid lines) and $b = 1$ (broken lines). We set $c = 0$, so the protein profiles are symmetric about the LE/LC boundary located at $u = 0$, where the lipid concentration profile as given by (23) has an inflection point. For vanishing stiffness of the protein distribution ($b \rightarrow 0$), the profiles have discontinuous slopes

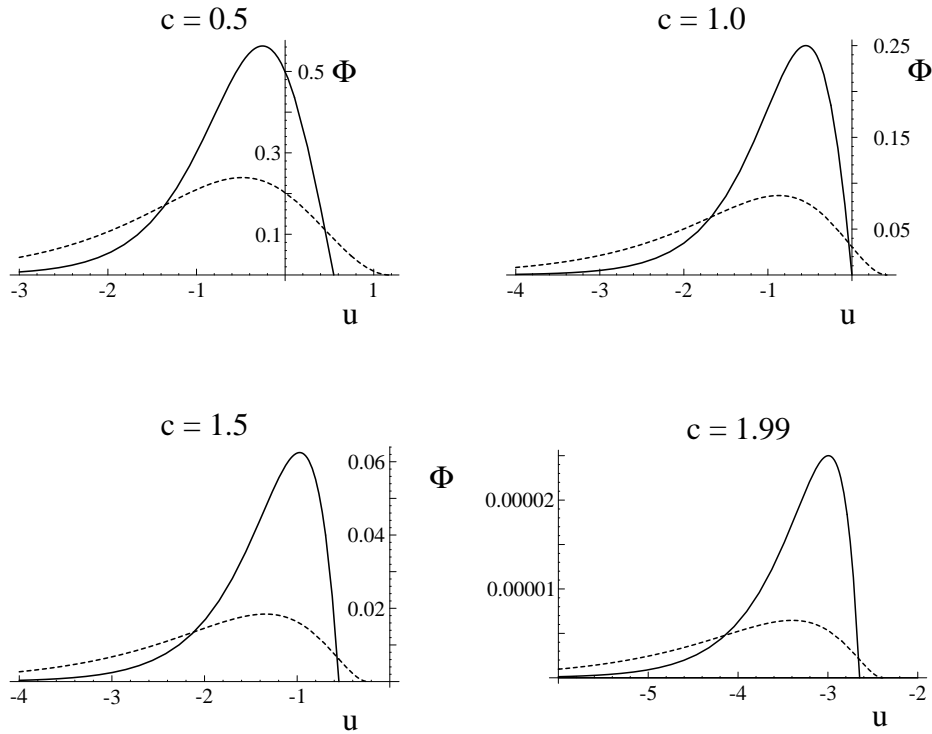


Fig. 4. — Asymmetric protein distributions at the boundary between the localized case and the semi-localized case, defined by $a = 1 - c$; solid lines denote $b = 0$ and broken lines denote $b = 1$. The left boundary u_1 is located at $u_1 = -\infty$ for all values of b .

for $a < 1$ at the points where the protein concentration vanishes; the main effect of a non-vanishing stiffness parameter b is to eliminate these discontinuities, thereby flattening the entire concentration profile, as is clearly seen in Figure 3.

Figure 4 shows asymmetric protein distributions for four different values of c on the transition line between the localized and the semi-localized regimes, defined by $a = 1 - c$. Again, solid lines denote results for $b = 0$ and broken lines denote results for $b = 1$. As for the symmetric distributions shown in Figure 3, a non-zero stiffness parameter b removes the discontinuity of $\Phi'(u)$ at the boundary u_2 and flattens the concentration profile. As c approaches the value 2, the maximum of the distribution moves progressively away from the LE/LC boundary located at $u = 0$. Also, the overall protein concentration rapidly decreases. In the limit $c \rightarrow 2$, the position of the maximum actually diverges logarithmically, as follows from (34).

Figure 5 gives the localized protein distribution $\Phi(u)$ for $c = 0$ and $a = 0.5$ for six different values of b , where u_2 and B have to be determined numerically from (42) applied to the general solution (31). Interestingly enough, the boundary values $u_2 = -u_1$ do not diverge as $b \rightarrow \infty$ but approach finite values $u_{1,2} = \mp 1.915$. As the stiffness of the protein distribution increases, the concentration is flattened and the area under the curves decreases, but the profile does not spread out indefinitely and stays localized.

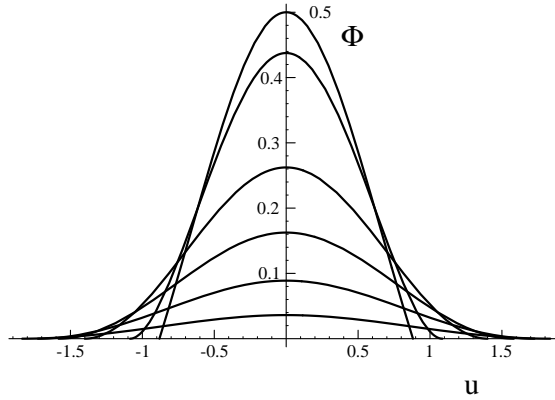


Fig. 5. — Protein distribution $\Phi(u)$ for vanishing lipid-protein interaction $c = 0$, and fixed protein chemical potential $a = 0.5$ for the following values of the protein stiffness b (from top to bottom): $b = 0, 0.2, 0.6, 1, 1.6$, and 2.8 . The limiting value of u_2 for $b \rightarrow \infty$ is given by $u_{1,2} = \pm 1.915$.

6. The Protein Excess

The protein excess is the total amount of adsorbed proteins. In the localized regime, this quantity is defined as

$$\Gamma \equiv \int_{-\infty}^{+\infty} \Phi(u) du = \int_{u_1}^{u_2} \Phi(u) du \quad (56)$$

In the delocalized and the semi-localized regimes, the quantity Γ as defined above diverges since the protein distribution approaches a constant non-vanishing value as $u \rightarrow -\infty$ (for the delocalized case the same is also true as $u \rightarrow \infty$). One can still extract a meaningful quantity defined by the excess amount of protein adsorbed by subtracting the protein concentration at $u = \pm\infty$, where $\Phi(\pm\infty) = a - 1 \mp c$. For $-2 < c < 2$ the protein distribution has one maximum, and we define the protein excess as

$$\Gamma \equiv \int_{-\infty}^{u_{\max}} (\Phi(u) - \Phi(-\infty)) du + \int_{u_{\max}}^{\infty} (\Phi(u) - \Phi(\infty)) du \quad (57)$$

where u_{\max} is the value of u for which $\Phi(u)$ reaches its maximum.

6.1. PROTEIN EXCESS FOR $b = 0$. — The protein excess Γ can be calculated for $b = 0$ in closed form for all parameter values. With $\Phi^0(u) = h(u) = a - \tanh^2(u) - c \tanh(u)$, the excess can be written as

$$\Gamma \equiv \int_{u_1}^{u_2} (a - \tanh^2(u) - c \tanh(u)) du \quad (58)$$

where the integration boundaries are given by

$$u_{1,2} = \tanh^{-1} \left[-\frac{c}{2} \mp \sqrt{\frac{c^2}{4} + a} \right] \quad (59)$$

For the symmetric case, $c = 0$, the boundaries u_1 and u_2 have the values

$$u_{1,2} = \mp \tanh^{-1} \sqrt{a} \quad (60)$$

and on the transition line between the localized and the semi-localized regimes, given by $a = 1 - c$, one obtains $u_1 = -\infty$ and

$$u_2 = \tanh^{-1}(1 - c) \quad (61)$$

For general a and c , the integral (58) yields

$$\Gamma = \sqrt{c^2 + 4a} + (a - 1 + c) \tanh^{-1} \left[\frac{\sqrt{c^2 + 4a}}{1 + a} \right] - c \tanh^{-1} \left[\frac{\sqrt{c^2 + 4a}(2 + c)}{2 + 2a + 2c + c^2} \right] \quad (62)$$

In the symmetric case, $c = 0$, this expression reduces to

$$\Gamma = (a - 1) \tanh^{-1} \left[\frac{\sqrt{4a}}{1 + a} \right] + \sqrt{4a} \quad (63)$$

and on the localized to semi-localized transition line, $a = 1 - c$, it reduces to

$$\Gamma = 2 - c - c \tanh^{-1} \left[\frac{4 - c^2}{4 + c^2} \right] = 2 - c - c \log(2/c) \quad (64)$$

Lines of constant Γ for $b = 0$ calculated from (62) are shown as broken lines in Figure 2. Those lines can be helpful in interpreting experimental findings when only the integrated protein amount is known and not the entire profile.

6.2. PROTEIN EXCESS FOR $b = 1$. — For the symmetric case ($c = 0$) the excess is given by the closed-form expression

$$\Gamma = 2(a - 1)u_2 + 2 \tanh u_2 \quad (65)$$

with the boundary value u_2 determined by

$$\tan^{-1}[\tanh(u_2/2)] = \frac{1 - a}{2} \sinh u_2 \quad (66)$$

as follows from (53) and (55) and noting that $A = 0$ in (31).

For the localized to semi-localized transition line, $a = 1 - c$, the excess is given by

$$\Gamma = 1 - c \log(2) + \tanh u_2 - u_2 c - c \log(\cosh u_2) \quad (67)$$

with the boundary value u_2 determined by

$$2c + 1 = \tanh u_2 + (1 + c)(\cosh u_2 - \sinh u_2)(\pi/2 + 2 \tan^{-1}(\tanh[u_2/2])) \quad (68)$$

as follows from applying (42) to (47).

The protein excess Γ for the symmetric case $c = 0$ is shown in Figure 6a as a function of a , where the solid line denotes results for $b = 0$ and the broken line for $b = 1$. These results correspond to the concentration profiles plotted in Figure 3 and are given by (63) and (65). The protein excess for $b = 1$ is smaller than for $b = 0$, which is also visible in Figure 3. The overall flattening of the distributions for non-zero b causes the area under the distribution to decrease. For $a = 1$, the protein excess is given by $\Gamma = 2$ for both values of b . The same value holds for general b , as can be demonstrated by numerical solutions of (56). The boundary values u_2 given by (60) for $b = 0$ and determined by (66) for $b = 1$ are plotted in Figure 7a.

In Figure 6b we show the protein excess on the localized/semi-localized transition line, $a = 1 - c$, as a function of c , as given by (64) and (67). As in the symmetric case, the protein excess Γ decreases as b becomes non-zero. The boundary values u_2 , obtained from (61) and (68), for $b = 0$ and $b = 1$, respectively, are plotted in Figure 7b.

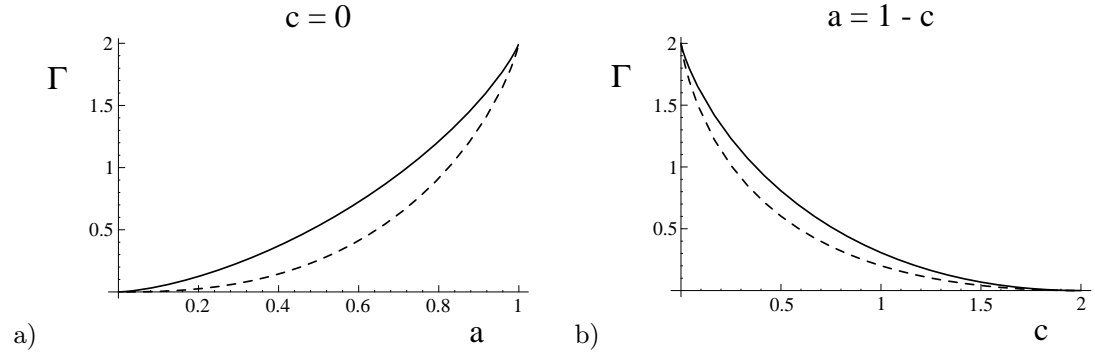


Fig. 6. — (a) Protein excess Γ for the symmetric case $c = 0$; the solid line denotes $b = 0$ and the broken line denotes $b = 1$. At $a = 1$ the excess is $\Gamma = 2$ independently of the value of b . (b) Protein excess Γ on the localized/semi-localized transition line, defined by $a = 1 - c$.

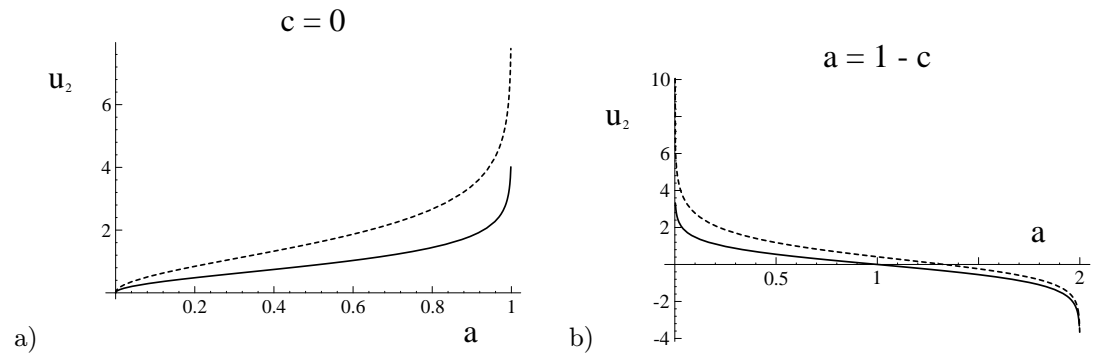


Fig. 7. — (a) Boundary value u_2 for the symmetric case $c = 0$ for $b = 0$ (solid line) as given by (60) and for $b = 1$ (broken line) as determined by (66); note that here $u_1 = -u_2$. (b) Boundary value u_2 for the localized to semi-localized transition line, defined by $a = 1 - c$, for $b = 0$ (solid line) as given by (61) and for $b = 1$ (broken line) as determined by (68); note that here $u_1 = -\infty$.

7. LE/LC Line Tension in the Presence of Protein

First we calculate the line tension of the liquid expanded-liquid condensed (LE-LC) interface in the absence of proteins, denoted by τ_0 . This energy per unit length follows from the total free energy density γ as given by (14) after subtraction of the bulk free energy density infinitely far from the interface and can be defined by

$$\frac{\tau_0}{2} = \int_0^\infty dx \left\{ -J\eta_0^2(x) + \frac{1}{12}\eta_0^4(x) + \frac{1}{2}g_\eta \left(\frac{d\eta_0(x)}{dx} \right)^2 + J\eta_\infty^2 - \frac{1}{12}\eta_\infty^4 \right\} \quad (69)$$

recalling that

$$\eta_0(x) = \eta_\infty \tanh(x/\xi_\eta) \quad (70)$$

and $\eta_\infty = \sqrt{6J}$ and $\xi_\eta = \sqrt{g_\eta/J}$. In writing (69) we used the symmetry around $x = 0$. The integral (69) is elementary and gives the standard result

$$\tau_0 = 8J^{3/2}g_\eta^{1/2} \quad (71)$$

The total line tension is given by $\tau = \tau_0 + \tau_\phi$. The line tension contribution τ_ϕ due to adsorbed proteins in the localized phase region can be written as

$$\tau_\phi = \int_{-\infty}^{\infty} dx \left\{ L\phi^2(x) - \mu\phi(x) + \lambda\eta_0(x)\phi(x) + \frac{1}{2}\eta_0^2(x)\phi(x) + \frac{1}{2}g_\phi \left(\frac{d\phi(x)}{dx} \right)^2 \right\} \quad (72)$$

For simplicity, we will restrict ourselves to the limit $g_\phi = 0$, because the integration in (72) can then be done in a closed form. The line tension contribution τ_ϕ can be expressed in reduced variables as

$$\tau_\phi = \frac{\xi_\eta \eta_\infty^4}{8L} \int_{-\infty}^{\infty} du \left\{ \frac{1}{2}\Phi^2(u) - a\Phi(u) + c \tanh u \Phi(u) + \tanh^2 u \Phi(u) \right\} \quad (73)$$

Using the solution found for $b = 0$ (or, equivalently, $\xi_\phi = 0$), $\Phi(u) = a - \tanh^2 u - c \tanh u$, the integral can be solved for general a and c . Here, we only present the solution for the symmetric case, $c = 0$, which is given by

$$\tau_\phi = \frac{9J^{3/2}g_\eta^{1/2}}{2L} \left\{ \sqrt{a}(1 - 5a/3) - (1 - a)^2 \tanh^{-1}(\sqrt{a}) \right\} \quad (74)$$

The limiting values are $\tau_\phi = 0$ for $a = 0$, since in this case no proteins are adsorbed, and $\tau_\phi = -3J^{3/2}g_\eta^{1/2}/L$ for $a = 1$, to be compared with $\tau_0 = 8J^{3/2}g_\eta^{1/2}$. This is the smallest value possible, for larger values of a the line tension contribution τ_ϕ remains constant. The adsorption of proteins thus leads to a reduction of the total line tension $\tau = \tau_0 + \tau_\phi$. In principle, the total line tension τ can take negative values for sufficiently large a if $L < 3/8$, which amounts to an instability of the LE-LC interface, possibly signaling a depression of the lipid phase transition. Of course, in this limit the approximations used in deriving (26) break down, since we assumed L to be large and the proteins being only a small perturbation on the pure lipid phase transition.

8. Protein Profile in the Subphase

Up to now the coupled protein-lipid system was considered as a pure two-dimensional system on the water/air interface which is positioned at $z = 0$. It is possible to evaluate the influence of a finite solubility of the proteins in the subphase on the protein distribution in the monolayer, and, in addition, to give a more precise meaning to the protein parameters μ and L used in (13). The vertical protein concentration profile in the subphase can be calculated as a function of the distance z from the monolayer. For the calculation of this profile, which is denoted by $\phi_\perp(z)$, we neglect any variation in the horizontal direction. Assuming that the water is a good solvent for the protein (and, therefore, that the aqueous protein solution is far from its demixing curve), we can write the free energy per unit area on the surface as

$$\gamma_\perp = \int_0^\infty dz \left\{ \frac{1}{2}g_\phi^b \left(\frac{d\phi_\perp(z)}{dz} \right)^2 + L_b\phi_\perp^2(z) - \mu_b\phi_\perp(z) \right\} + L_s\phi^2 - \mu_s\phi \quad (75)$$

where $\phi = \phi_\perp(0)$ is the protein concentration at the surface (or, equivalently, in the monolayer). This expression is very similar to free energy functionals studied in the context of wetting and other surface phenomena [30]. In analogy to the parameters used in (13) and (15), g_ϕ^b , L_b , and μ_b are the protein parameters in the ‘‘bulk’’ subphase, and L_s and μ_s are the bare protein parameters at the ‘‘surface’’ (or in the monolayer). The chemical potential μ_s measures the

free energy difference between a protein molecule in the subphase and in the monolayer, and it contains contributions due to van der Waals interactions of the protein with its surrounding media as well as hydrophobic contributions coming from structural changes of the protein at the surface. It is believed that proteins unfold their hydrophobic parts when they are inside a monolayer or even at the free air-water interface. The energy gained by such conformational transformations can be extremely high.

The Euler-Lagrange equation for the bulk density profile takes the form

$$2L_b\phi_{\perp}(z) - \mu_b = g_{\phi}^b \frac{d^2\phi_{\perp}(z)}{dz^2} \quad (76)$$

The bulk protein concentration infinitely far from the monolayer is given from (76) by

$$\phi_b \equiv \phi_{\perp}(\infty) = \frac{\mu_b}{2L_b} \quad (77)$$

When the protein adsorbing on the surface is in contact with a large bulk reservoir of proteins, the bulk concentration ϕ_b can be regarded as a fixed parameter and the chemical potential μ_b acts as a Lagrange multiplier satisfying the relation $\mu_b = 2L_b\phi_b$.

The solution of (76) compatible with the requirement $\phi_{\perp}(\infty) = \phi_b$ is given by

$$\phi_{\perp}(z) = (\phi - \phi_b)e^{-z/\xi_{\phi}^b} + \phi_b \quad (78)$$

where the correlation of the protein distribution in the subphase is $\xi_{\phi}^b = \sqrt{g_{\phi}^b/2L_b}$ and $\phi \equiv \phi_{\perp}(0)$ is the surface value. The surface free energy, which is the total free energy due to the presence of the monolayer at $z = 0$, can be expressed as

$$\Delta\gamma_{\perp} = \gamma_{\perp} - \int_0^{\infty} dz \{L_b\phi_b^2 - \mu_b\phi_b\} \quad (79)$$

For the density profile given by (78), it takes the form

$$\Delta\gamma_{\perp} = (\phi - \phi_b)^2 \sqrt{L_b g_{\phi}^b / 2} + L_s \phi^2 - \mu_s \phi \quad (80)$$

Minimizing this expression with respect to the surface protein concentration ϕ leads to the value

$$\phi = \frac{\mu_s + \phi_b \sqrt{2L_b g_{\phi}^b}}{2L_s + \sqrt{2L_b g_{\phi}^b}} \quad (81)$$

Effectively, the presence of a finite concentration of proteins in the subphase can be modeled by using the modified parameters

$$\mu = \mu_s + \phi_b \sqrt{2L_b g_{\phi}^b} \quad (82)$$

$$L = L_s + \sqrt{L_b g_{\phi}^b / 2} \quad (83)$$

for the two-dimensional description of the protein distribution in the monolayer, given in (13). With these effective parameters, the ϕ -dependent part of the surface free energy can be rewritten (up to a constant) as $\Delta\gamma_{\perp} = L\phi^2 - \mu\phi$. For very large values of the protein adsorption free energy μ_s , as observed for proteins which change their structure considerably as they

approach the air-water interface, and a rather small reservoir of proteins in the subphase, most of the proteins will be incorporated in the monolayer leading to a depletion in the subphase, *i.e.*, $\phi_b \approx 0$. In this case the total amount of protein in the monolayer is a conserved quantity and μ then acts as a Lagrange multiplier. In the case of a large reservoir of proteins in the subphase, conservation of protein particles is taken care of primarily by adjusting the bulk concentration ϕ_b . In both cases, the parameter μ , which appears in (13), can be tuned by changing the total amount of protein added to the system.

9. Surface Pressure

We discuss now how the parameters used in our calculation can be related to experimentally measurable quantities, such as the lateral pressure Π . This will be done for the simplified cases where there are either only proteins or only lipids at the water surface. We calculate the lateral pressure in the limit of small coverage with proteins or lipids, leading to a modified ideal gas law; the correction to the limiting ideal gas behavior gives information about the interactions.

In the case where no lipid is present at the water surface, one sets $\eta = \phi - 1$ in (7) and the free energy per lattice site (neglecting linear terms in the protein concentration ϕ) is

$$\mathcal{F}(\phi)/T = K\phi^2 + \frac{\phi}{\alpha} \log\left(\frac{\phi}{\alpha}\right) + (1 - \phi) \log(1 - \phi) - (1 - \phi + \frac{\phi}{\alpha}) \log(1 - \phi + \frac{\phi}{\alpha}) \quad (84)$$

where α is the area ratio of the protein and the underlying lipid/vacancy lattice. $K \equiv L + \lambda - J - 1/2$ is an effective interaction parameter. For the case where only lipids are present one has to make the replacements $K \rightarrow -4(J + 1/2)$, $\phi \rightarrow \phi_L$ and $\alpha \rightarrow 1$. The thermodynamic potential for a system covering N lattice sites is defined by

$$N\mathcal{G} = N\mathcal{F} - \mu TN\phi + \Pi Na^2 \quad (85)$$

with a being the lattice constant of the underlying lattice of vacancies or lipids. Minimizing the potential with respect to the number of occupied lattice sites N and the protein density ϕ leads to

$$\mu = \left. \frac{d\mathcal{F}(\phi)/T}{d\phi} \right|_{\phi=\phi_{\text{eq}}} \quad (86)$$

$$-\mathcal{F}(\phi_{\text{eq}}) + \mu T\phi_{\text{eq}} = \Pi a^2 = \phi^2 \left. \frac{d\mathcal{F}(\phi)/\phi}{d\phi} \right|_{\phi=\phi_{\text{eq}}} = TK\phi_{\text{eq}}^2 - T \log(1 - \phi_{\text{eq}}) + T \log(1 - \phi_{\text{eq}} + \phi_{\text{eq}}/\alpha) \quad (87)$$

Expanding the logarithm, one finds the behavior valid for small surface pressures

$$\Pi A = T + A^{-1} a^2 \alpha T (1 + \alpha K - 1/2\alpha) \simeq T + \Pi a^2 \alpha (1 + \alpha K - 1/2\alpha) \quad (88)$$

where $A = a^2 \alpha / \phi_{\text{eq}}$ is the surface area available per protein (or lipid if one makes the replacement $\alpha = 1$). The first term in (88) corresponds to the ideal gas behavior, the second term is an enthalpic and entropic correction from which the effective interaction term K can be deduced, if the area of a protein, $a^2 \alpha$, and the protein-lipid area ratio α are known.

Measurements of ΠA as a function of Π for the hydrophobic polypeptide *cyclosporin A* in the relevant temperature range showed positive slopes [21], indicative of an interaction parameter K far above the critical value. The sign of the parameter λ indicates the preference for the protein to enter dense ($\lambda < 0$) or dilute lipid regions ($\lambda > 0$); experiments indicate that this parameter is close to zero, so that L is larger than zero. Neglecting higher-order terms in ϕ in

the free energy expression (13) thus seems justified, assuming that *cyclosporin A* is a typical protein.

For fitting experimental data to the above expression it is important to note that the interaction parameters J , L , and λ as defined by (9-11) depend on the temperature.

10. Discussion

We studied a simple model which explains possible aggregation of proteins or other large macromolecules at the boundary between coexisting liquid condensed and liquid expanded domains of lipids. Such a preferential adsorption of proteins has been observed experimentally [22]. Based on the general phase diagram, shown in Figure 2, obtained in the limit of proteins with large areas compared with lipids ($\alpha \rightarrow \infty$), we predict a transition from protein distributions localized at the LE/LC boundary to semi-localized and delocalized distributions, for which the protein concentrations remain non-zero in the coexisting lipid phases. Such a transition can be observed by either changing the total amount of adsorbed proteins (corresponding to a change in a), or by changing the temperature (influencing the parameter c). We also calculated various experimentally accessible quantities, such as the protein excess Γ and the LE-LC line tension τ . The line tension is predicted to decrease upon adsorption of proteins.

The mechanism leading to the preferential adsorption of proteins at the one-dimensional boundary line between LE and LC phases is due to a competition of the different contributions to the entropy of mixing of the three components: proteins, lipids, and vacancies. We recall that vacancies are artificially introduced just to allow the Langmuir monolayer to be compressible. Our model assumes that the protein actually penetrates into the monolayer. A partial intrusion is also possible and can be described by the model, if the proteins take up at least some area at the air-water interface. Other mechanisms based on long-ranged interactions such as electrostatic forces are also important and could lead to similar results.

The affinity of the proteins to the LE/LC boundary can also originate from other enthalpic reasons: If the protein itself has amphiphilic properties with respect to the density of the surrounding medium, *i.e.*, if one moiety of the protein favors a denser environment while the other moiety favors a more dilute environment, it would be driven into the interface between the LE and LC phases. However, such an amphiphilic property of the proteins seems to be unlikely, and, if present, too weak to produce the effects observed in experiments.

Finally, we mention that similar effects should be observable for freely suspended multicomponent membranes which show phase separation into coexisting domains with different lipid compositions [2, 25, 26]. Here, integral membrane proteins should be either dissolved in one of the domains, depending on the enthalpic preference, or, if this preference is very weak, enriched and localized at the one-dimensional boundary line between the domains.

Acknowledgments

We would like to thank A. Goudot, H. Möhwald, E. Sackmann, M. Schick, and T. Schwinn for helpful discussions. DA acknowledges partial support from the German Israel Foundation (GIF) under grant No. I-0197 and the US-Israel Binational Science Foundation (BSF) under grant No. 94-00291. RN acknowledges support from the Minerva Foundation, receipt of a NATO stipend administered by the DAAD, and partial support by the National Science Foundation under Grant No. DMR-9531161.

Appendix A

Solution of Differential Equation

Here we derive the solution of the differential equation

$$\Phi(u) - h(u) = b^2 \frac{d^2 \Phi(u)}{du^2} \quad (\text{A.1})$$

with the inhomogeneous term $h(u)$ given by

$$h(u) \equiv a - \tanh^2 u - c \tanh u \quad (\text{A.2})$$

Denoting by Φ_A and Φ_B two independent solutions of the homogeneous differential equation $\Phi(u) = b^2 \Phi''(u)$, the particular solution of the inhomogeneous differential equation is formally given by

$$\Phi_P(u) = -\frac{1}{b^2} \int_0^u dw h(w) \frac{\Phi_A(w)\Phi_B(u) - \Phi_A(u)\Phi_B(w)}{\Phi_A(w)\Phi_B'(w) - \Phi_A'(w)\Phi_B(w)} \quad (\text{A.3})$$

Choosing $\Phi_A(u) = A \sinh(u/b)$, $\Phi_B(u) = B \cosh(u/b)$, and defining the particular solution as

$$\Phi_P(u) = a - \frac{1}{b} \Phi_1(u) - \frac{c}{b} \Phi_2(u) \quad (\text{A.4})$$

the integrals to be solved are

$$\Phi_1(u) \equiv \int_0^u dw \tanh^2(w) \sinh\left(\frac{w-u}{b}\right) \quad (\text{A.5})$$

$$\Phi_2(u) \equiv \int_0^u dw \tanh(w) \sinh\left(\frac{w-u}{b}\right) \quad (\text{A.6})$$

The integration is straightforward and yields

$$\begin{aligned} \Phi_1(u) &= b - b \cosh(u/b) + \sinh(u/b) \\ &+ \frac{1}{4b} e^{-u/b} \left(\Psi \left[\frac{1}{2} + \frac{1}{4b} \right] - \Psi \left[\frac{1}{4b} \right] \right) + \frac{1}{4b} e^{u/b} \left(\Psi \left[\frac{1}{2} - \frac{1}{4b} \right] - \Psi \left[-\frac{1}{4b} \right] \right) \\ &+ 2bF \left[2; -\frac{1}{2b}; 1 - \frac{1}{2b}; -e^{2u} \right] + 2bF \left[2; \frac{1}{2b}; 1 + \frac{1}{2b}; -e^{2u} \right] \\ &- 2bF \left[1; -\frac{1}{2b}; 1 - \frac{1}{2b}; -e^{2u} \right] - 2bF \left[1; \frac{1}{2b}; 1 + \frac{1}{2b}; -e^{2u} \right] \end{aligned} \quad (\text{A.7})$$

$$\begin{aligned} \Phi_2(u) &= b - b \cosh(u/b) \\ &+ \frac{1}{4} e^{-u/b} \left(\Psi \left[\frac{1}{2} + \frac{1}{4b} \right] - \Psi \left[\frac{1}{4b} \right] \right) - \frac{1}{4} e^{u/b} \left(\Psi \left[\frac{1}{2} - \frac{1}{4b} \right] - \Psi \left[-\frac{1}{4b} \right] \right) \\ &- bF \left[1; -\frac{1}{2b}; 1 - \frac{1}{2b}; -e^{2u} \right] - bF \left[1; \frac{1}{2b}; 1 + \frac{1}{2b}; -e^{2u} \right] \end{aligned} \quad (\text{A.8})$$

where $\Psi[z]$ denotes the *digamma function* and $F[\alpha; \beta; \gamma; z]$ denotes the *hypergeometric function* [31]. These special functions are defined by

$$\Psi[z] = \frac{d[\log(\Gamma[z])]}{dz} \quad (\text{A.9})$$

with the gamma function defined as usual as

$$\Gamma[z] = \int_0^{\infty} t^{z-1} e^{-t} dt \quad (\text{A.10})$$

and

$$F[\alpha; \beta; \gamma; z] = \frac{\Gamma[\gamma]}{\Gamma[\beta]\Gamma[\gamma-\beta]} \int_0^1 t^{\beta-1} (1-t)^{\gamma-\beta-1} (1-tz)^{-\alpha} dt \quad (\text{A.11})$$

For the special case $b = 1$, the above expressions simplify and can be expressed as

$$\Phi_1(u) = 2 - 2 \cosh(u) + 2 \tan^{-1}[\tanh(u/2)] \sinh(u) \quad (\text{A.12})$$

$$\Phi_2(u) = \sinh(u) - 2 \tan^{-1}[\tanh(u/2)] \cosh(u) \quad (\text{A.13})$$

The general solution of the differential equation is given by

$$\Phi(u) = A \sinh(u/b) + B \cosh(u/b) + a - \Phi_1(u)/b - c \Phi_2(u)/b \quad (\text{A.14})$$

where the constants A and B are determined from the boundary conditions (see text).

Appendix B

Low Protein Concentration Expansion

Here we discuss the validity of the approximations leading from the Euler-Lagrange equations (21) and (22) to the differential equation (26). Namely, the use of the solution $\eta_0(x)$ in (22) which was obtained by neglecting the two terms $\lambda\phi$ and $\eta\phi$ in (21). The solution $\eta_0(x)$ of the simplified differential equation obtained by setting $\phi = 0$ in (21) can be regarded as a zeroth-order approximation to the full solution in an expansion in powers of $\phi(x)$. The validity of this approximation can be estimated by reconsidering the differential equation (21) and substituting for ϕ the solution $\phi(x)$ which was found initially by neglecting the coupling terms between η and ϕ in (21).

Consider first the second coupling $\eta\phi$ between ϕ and η in (21). This term is unimportant as long as $\phi \ll J$. This is a reasonable assumption given that the protein concentration is small and one is not too close to the critical point of the liquid-expanded liquid-condensed lipid transition. This term will not be considered any further.

In order to estimate the effect of the other term which was neglected, $\lambda\phi$, we define

$$\eta(x) \equiv \eta_0(x) + \delta\eta(x) \quad (\text{B.1})$$

with $\eta_0(x)$ given by (23) and $\eta(x)$ denoting the exact solution of (21). Since $\eta_0(x)$ solves equation (21) without the terms proportional to ϕ , the differential equation for $\delta\eta(x)$ neglecting terms of $\mathcal{O}(\delta\eta^2, \delta\eta\phi)$ is given by

$$\delta\eta(x)(-2J + \eta_0^2(x)) + \phi(x)(\lambda + \eta_0(x)) = g_\eta \delta\eta''(x) \quad (\text{B.2})$$

From the differential equation (21), one sees that the correction we are estimating here is important only for

$$\lambda\phi \gg |-2J\eta_0 + \eta_0^3/3| \simeq |-2J\eta_0| \quad (\text{B.3})$$

The last step follows since $\eta_0(x)$ has to be much smaller than unity for the inequality to hold. This can only be true in the close vicinity to the interface between dense and dilute lipid regions, *i.e.*, for $x \approx 0$. Consequently, the correction $\delta\eta(x)$ is only important around $x = 0$.

Then, the terms proportional to $\eta_0(x)$ can be neglected and the differential equation (B.2) simplifies to

$$-2J\delta\eta(x) + \lambda\phi(x) = g_\eta\delta\eta''(x) \quad (\text{B.4})$$

Replacing $\phi(x)$ by its value at the origin, $\phi(0)$, the solution of (B.4) is formally written as

$$\delta\eta(x) = \frac{\lambda\phi(0)}{2J} + C \sin(\sqrt{2}x/\xi_\eta) + D \cos(\sqrt{2}x/\xi_\eta) \quad (\text{B.5})$$

In order for the correction $\delta\eta(x)$ to vanish outside the region of interest centered around $x \approx 0$, both coefficients C and D have to be of the order as the constant $\lambda\phi(0)/2J$. The magnitude of the correction is thus given by

$$\delta\eta \simeq \frac{\lambda\phi(0)}{J} \sim \frac{c\phi(0)}{\eta_\infty} \quad (\text{B.6})$$

Note that c is a parameter of order unity (or smaller) in the localized protein region (see Fig. 2). Thus, the correction $\delta\eta$ enters in the calculation of the protein distribution $\phi(x)$ as a higher order contribution in terms of the ratio $\phi(0)/\eta_\infty$, which is a small parameter. Neglecting this correction is a controlled approximation corresponding to keeping only the first order in a general expansion in terms of $\phi(0)/\eta_\infty$, the ratio of the protein concentration and the lipid concentration difference.

References

- [1] Gaines G.L. Jr., *Insoluble Monolayers at Liquid-Gas Interfaces* (Interscience, New York, 1966).
- [2] Bloom M., Evans E. and Mouritsen O.G., *Quart. Rev. Biophys.* **24** (1991) 293.
- [3] For recent reviews, see Möhwald H., *Annu. Rev. Phys. Chem.* **41** (1990) 441; McConnell H.M., *Annu. Rev. Phys. Chem.* **42** (1991) 171; Knobler C.M., *Adv. Chem. Phys.* **77** (1990) 397; Andelman D., Brochard F., Knobler C. and Rondelez F., in *Micelles, Membranes, Microemulsions, and Monolayers*, W.M. Gelbart, A. Ben-Shaul and D. Roux Eds. (Springer-Verlag, Berlin, 1994).
- [4] Albrecht O., Gruler H. and Sackmann E., *J. Phys. France* **39** (1978) 301.
- [5] Albrecht O., Gruler H. and Sackmann E., *J. Colloid Interface Sci.* **79** (1981) 319.
- [6] Möhwald H., *Thin Solid Films* **159** (1988) 1; Kjaer K., Als-Nielsen J., Helm C.A., Tippmann-Krayer P., and Möhwald H., *J. Chem. Phys.* **93** (1989) 3200; Möhwald H., Kenn R.M., Degenhardt D., Kjaer K. and Als-Nielsen J., *Physica A* **168** (1991) 127; Kenn R.M., Böhm C., Bibo A.M., Peterson I.R., Möhwald H., Als-Nielsen J. and Kjaer K., *J. Chem. Phys.* **95** (1991) 2092.
- [7] Barton S.W., Thomas B.N., Flom E.B., Rice S.A., Lin B., Penn J.B., Ketterson J.B. and Dutta P., *J. Chem. Phys.* **89** (1988) 5898; Lin B., Penn J.B., Ketterson J.B., Dutta P., Thomas B.N., Buontempo J. and Rice S.A., *J. Chem. Phys.* **90** (1989) 2393; Lin B., Shih M.C., Bohanon T.M., Ice G.E., Dutta P., *Phys. Rev. Lett.* **65** (1990) 191.
- [8] Barton S., Goudot A., Bouloussa O., Rondelez F., Lin B., Novak F., Acero A. and Rice S.A., *J. Chem. Phys.* **96** (1992) 1343.
- [9] Schlossmann M.L., Schwartz D.K., Pershan P.S., Kawamoto E.H., Kellog G.J. and Lee S., *Phys. Rev. Lett.* **66** (1991) 1599.

- [10] Grundy M.J., Richardson R.M., Roser S.J., Penfold J. and Ward R.C., *Thin Solid Films* **159** (1988) 43.
- [11] Bibo A.M., Knobler C.M. and Peterson I.R., *J. Chem. Phys.* **95** (1991) 5591.
- [12] Pallas N.R. and Pethica B.A., *Langmuir* **1** (1985) 509; Earnshaw J.C. and Winch P.J., *J. Phys.: Cond. Matter* **2** (1990) 8499.
- [13] McConnell H.M., Keller D. and Gaub H., *J. Phys. Chem.* **90** (1986) 1717; Keller D.J., Korb J.P. and McConnell H.M., *ibid.* **91** (1987) 6417; McConnell H.M. and Moy V.T., *ibid.* **92** (1988) 4520; Miller A. and Möhwald H., *J. Chem. Phys.* **86** (1987) 4258; Knobler C.M., *Science* **249** (1990) 870.
- [14] Marčelja S., *Biochim. Biophys. Acta* **367** (1974) 165.
- [15] Earlier theories are reviewed in Bell G.M., Combs L.L. and Dunne L.J., *Chem. Rev.* **81** (1981) 15.
- [16] Georgallas A. and Pink D.A., *J. Colloid Interface Sci.* **89** (1982) 107; Roland C.M., Zuckermann M.J. and Georgallas A., *J. Chem. Phys.* **86** (1987) 5812.
- [17] Chen Z.-Y., Talbot J., Gelbart W.M. and Ben-Shaul A., *Phys. Rev. Lett.* **61** (1988) 1376.
- [18] Kramer D., Ben-Shaul A., Chen Z.-Y. and Gelbart W.M., *J. Chem. Phys.* **96** (1992) 2236.
- [19] von Tschärner V. and McConnell H.M., *Biophys. J.* **36** (1981) 409; Lösche M., Sackmann E. and Möhwald H., *Ber. Bunsenges. Phys. Chem.* **87** (1983) 848; Peters R. and Beck K., *Proc. Natl. Acad. Sci. USA* **80** (1983) 7183; Weiss R.M. and McConnell H.M., *Nature* **310** (1984) 5972; Lösche M. and Möhwald H., *Rev. Sci. Instrum.* **55** (1984) 1968.
- [20] Hénon S. and Meunier J., *Rev. Sci. Instrum.* **62** (1991) 936; Hönig D. and Möbius D., *J. Phys. Chem.* **91** (1991) 4590.
- [21] Wiedmann T.S. and Jordan K.R., *Langmuir* **7** (1991) 318.
- [22] Schwinn T., Diploma Thesis (Technical University of Munich, 1992) unpublished.
- [23] Vogel V., in *Proteins at Interfaces*, T.A. Horbett and J.L. Brash Eds. (ACS Books, in press).
- [24] Haas H., Diploma Thesis (University of Mainz, 1988) unpublished; Haas H. and Möhwald H., *Thin Solid Films* **180** (1989) 101.
- [25] Thewalt J.L. and Bloom M., *Biophys. J.* **63** (1992) 1176.
- [26] Wu S.H.-W. and McConnell H.M., *Biochemistry* **14** (1975) 847.
- [27] It turns out that taking the limit $\alpha \rightarrow \infty$ corresponds to neglecting the entropy contribution from the proteins while maintaining $\phi \geq 0$, *i.e.*, keeping a positive protein concentration.
- [28] Halperin A. and Pincus P., *Macromolecules* **19** (1986) 79.
- [29] Two-phase coexistence is observed on a whole line in the chemical-potential plane (μ_η, μ) ; three-phase coexistence, which occurs for small or negative values of L and large values of ϕ , is not considered here.
- [30] Brézin E., Halperin B.I. and Leibler S., *J. Phys. France* **44** (1983) 775.
- [31] Handbook of Mathematical Functions, Chapter 15, M. Abramowitz and I.A. Stegun Eds. (Dover, New York, 1972).